Electromagnetic Analysis of Arbitrary Antennas on Large Composite Platforms Using PO Driven MoM

Miodrag S. Tasic[1], Branko M. Kolundzija[2]

Abstract – **Electromagnetic analysis of electrically large problems using numerically exact method of moments (MoM) is enormous burden for a personal computer. So called fast techniques cut down CPU time, but storage problem remains. Here we present novel iterative method which converges toward MoM solution, but does not deal with large matrices. The method is especially suitable for isolated antennas on large objects.**

Keywords – **Electromagnetic analysis, Method of moments, Antennas, Physical optics.**

I. INTRODUCTION

Surface integral equations (SIEs) of electromagnetic field in frequency domain can be solved using method of moments (MoM) [1]. MoM transforms SIEs into a system of linear equations, which unknowns are weighting coefficients of adopted basis functions (BFs). MoM solution is expressed as a finite series (linear combination of BFs) so, essentially, it is approximate. However, by proper choice of BFs, the solution converges toward exact solution when number of BFs increases, i.e. it is numerically exact. The main drawback of MoM is poor scalability - the number of BFs per wavelength squared is fixed, hence total number of BFs (N) raising fast by increasing frequency. Furthermore, memory occupancy is $O(N^2)$, and CPU solution time is $O(N^3)$. So, there is a clear limit on a electrical size of problems that can be solved using certain computer.

There are a number of techniques for accelerating MoM: hybridization with asymptotic methods [2,3], fast multipole method [4,5], compression of MoM matrix [6]. For all of them, at some point, the entire MoM matrix should be available. So, while these methods cut down CPU time, the storage remains the bottleneck. Another approach is use of characteristic basis functions, suitable for the problem particular geometry [7,8]. In [9] we proposed technique which has some similarities with such approach. It is iterative method which converges toward MoM solution by employing correctional currents created in physical optics (PO) manner. (That is why the method was called PO driven MoM – PDM). These currents are then used to create macro basis functions, appropriate for that particular structure. PDM does not need to store entire MoM matrix at once, or to deal with it as a whole. This way, PDM significantly decreases memory occupancy and CPU time, while preserving sufficient accuracy.

[1]Miodrag S. Tasic is with the School of Electrical Engineering, University of Belgrade, Bulevar kralja Aleksandra 73, 11120 Belgrade, Serbia, E-mail: tasic@etf.rs

[2]Branko M. Kolundzija is with the School of Electrical Engineering, University of Belgrade, Bulevar kralja Aleksandra 73, 11120 Belgrade, Serbia, E-mail: kol@etf.rs

In [9], PDM is formulated as a method for analyzing perfectly conducting (PEC) closed scatterers (and particularly well suited for electrically large problems). In [10,11] we introduced some modifications in the PDM method, considering adaptive grouping and analysing composite scatteres, made of metal and dielectric.

In [12] we presented some results for PDM applied to antenna problems, but without details of the theory of operation. Complete theory of PDM applied to antenna problems was first described in [13]. Here we extend that work. The essence of the method is the same as for the scatterers – we add new macro basis functions (MBFs) in each iteration and adjust their weighting coefficients to minimize the difference between PDM and MoM solution. However, only perfectly conducting parts that belong to closed surfaces can be treated in "modified PO" way [9], whereas MBFs in the rest of the structure are obtained using new approach, discussed here.

Theory of PDM applied to antenna problems is given in section II, numerical examples in section III, and conclusion in section IV.

II. PDM APPLIED TO ANTENNA PROBLEMS

We start from an existing MoM solution of surface integral equations. Unknown vector function $\mathbf{f}$ is approximated by linear combination ($\mathbf{f}_\mathrm{a}$) of N known vector BFs ($\mathbf{f}_k$) multiplied by unknown complex scalar coefficients (a_k)

$$\mathbf{f}_\mathrm{a} = \sum_{k=1}^{N} a_k \mathbf{f}_k \,. \tag{1}$$

Coefficients a_k are obtained from the MoM system of equations

$$\sum_{k=1}^{N} z_{jk} a_k = v_j, \quad j = 1,\ldots,N \tag{2}$$

where z_{jk} and v_j are known complex scalars.

In PDM, coefficients a_k are obtained in iterative manner. In ith iteration we determine one set of values, $a_k^{(i)}$ (for all coefficients, or some of them), and, using them, build $M^{(i)}$ MBFs, $\mathbf{F}_l^{(i)}$

$$\mathbf{F}_l^{(i)} = \sum_{k=1}^{N} b_{lk}^{(i)} a_k^{(i)} \mathbf{f}_k , \quad l = 1,...,M^{(i)} . \tag{3}$$

Coefficient $b_{lk}^{(i)}$ ($0 \le b_{lk}^{(i)} \le 1$) controls membership of *k*th BF to *l*th MBF in *i*th iteration. Initial solution is referenced as 0th iteration. Coefficients $a_k^{(i)}$ will be called *initial* coefficients for $i = 0$ and *correctional* coefficients for $i > 0$. PDM solution in *n*th iteration is adopted as

$$\mathbf{f}_\mathrm{a}^{(n)} = \sum_{i=0}^{n} \sum_{l=1}^{M^{(i)}} c_{il}^{(n)} \mathbf{F}_l^{(i)} , n > 0 , \tag{4}$$

where $c_{il}^{(n)}$ are unknown coefficients that should be determined. By substituting expression for $\mathbf{F}_l^{(i)}$ from (3) to (4), after some rearrangements, (4) can be expressed as

$$\mathbf{f}_\mathrm{a}^{(n)} = \sum_{k=1}^{N} A_k^{(n)} \mathbf{f}_k . \tag{5}$$

Expression (5) is formally the same as (1), except that coefficients $A_k^{(n)}$ do not satisfy MoM system (2). Instead, for each of equations in (2) we can define residual error

$$R_j^{(n)} = v_j - \sum_{k=1}^{N} z_{jk} A_k^{(n)} , \tag{6}$$

and mean value for all residual errors - Residuum

$$R^{(n)} = \frac{1}{N} \sum_{j=1}^{N} \left| R_j^{(n)} \right|^2 = \frac{1}{N} \left| v_j - \sum_{i=0}^{n} \sum_{l=1}^{M^{(i)}} c_{il}^{(n)} Z_{jl}^{(i)} \right|^2 , \tag{7}$$

where we introduced auxiliary "matrix"

$$Z_{jl}^{(i)} = \sum_{k=1}^{N} z_{jk} b_{lk}^{(i)} a_k^{(i)} . \tag{8}$$

Coefficients $c_{il}^{(n)}$ are determined in a way to minimize Residuum (7). By imposing condition

$$\frac{\partial R^{(n)}}{\partial c_{km}^{(n)}} = 0, \quad k = 0,..,n \quad m = 1,..,M^{(i)} , \tag{9}$$

we obtain PDM system of equations

$$\sum_{i=0}^{n} \sum_{l=1}^{M^{(i)}} c_{il}^{(n)} \left(\sum_{j=1}^{N} Z_{jl}^{(i)} Z_{jm}^{(k)*} \right) = \sum_{j=1}^{N} v_j Z_{jm}^{(k)*} . \tag{10}$$
$$k = 0,...,n, \quad m = 1,...,M^{(i)}$$

As a solution of the system (10) we obtain coefficients $c_{il}^{(n)}$. Note that, for efficient calculation of elements of PDM matrix (in (10) given by expression in the bracket), we do not need to know entire MoM matrix at once, but only a single row at once. Hence, if the MoM matrix is large, instead of calculating it one time and store it, we can calculate it in each iteration, one row at a time, thus decreasing memory demands from $O(N^2)$ to $O(N)$. In all practical situations order of the PDM matrix is by few orders smaller than order of the MoM matrix.

BFs are separated in two areas. BFs defined over PEC surfaces that are part of a closed surface can belong to PO area. All other BFs must be in MoM area. These two areas differ in a way that MBFs are created. For simplicity, we will assume that single MoM area exists and that first N_MoM BFs belong to it, whereas the rest of BFs belong to the PO area.

In PO area we determine correctional currents [2] in *i*th iteration just below the surface *S* of the structure (i.e. at S^-)

$$\Delta \mathbf{J}_\mathrm{s}^{(i)} = 2\mathbf{n} \times \mathbf{H}_\mathrm{tot}^{(i-1)}(\mathbf{r}), \mathbf{r} \in S^- , \tag{11}$$

and approximate these currents using BFs from PO area [2], i.e. we obtain correctional coefficients $a_k^{(i)}$

$$\Delta \mathbf{J}_\mathrm{s}^{(i)} \cong \sum_{k=N_\mathrm{MoM}+1}^{N} a_k^{(i)} \mathbf{f}_k . \tag{12}$$

Correctional currents determined in this way locally cancel magnetic field that exists within PEC part of the structure (whereas it should be zero). This approach has no meaning outside closed PEC region, i.e. in the MoM area. By formal extraction of MoM area from MoM system of equations we obtain partial system of equations. Correctional coefficients in MoM area are obtained using residual errors from previous iteration as excitation for partial system of equations, i.e.

$$\sum_{k=1}^{N_\mathrm{MoM}} z_{jk} a_k^{(i)} = R_j^{(i-1)}, \quad j = 1,..,N_\mathrm{MoM} . \tag{13}$$

Initial coefficients $a_k^{(0)}$ are obtained by solving partial system of equations

$$\sum_{k=1}^{N_\mathrm{MoM}} z_{jk} a_k^{(0)} = v_j , \quad j = 1,..,N_\mathrm{MoM} . \tag{14}$$

If the case of multiple MoM areas, we solve partial systems of equations (13) and (14) for each of them. Such situation can occur if we have multiple antennas mounted on the platform, far from each other, or we have dielectric parts on otherwise metal platform (composite platform). One MoM zone that includes all these parts can be too large and thus ineffective, so it is the best to have one MoM area for each isolated part that cannot be in the PO Area.

III. Numerical Examples

The first example is microstrip patch antenna (MPA) mounted on perfectly conducting, 59 wavelengths long, helicopter. The helicopter's nose is directed along –*x*-axis of Descartes coordinate system, whereas *z*-axis is orthogonal to helicopter's floor and directed toward its propeller. The structure is modeled using 12022 surface bilinear patches. MoM settings from [14,15] are adopted, i.e. we use polynomial higher order vector BFs. For this model, second order BFs are predominantly used, resulting in totally 95730 BFs. BFs can be defined over single patch or over more patches. MoM area includes MPA and certain number of neighboring patches. Patches in PO area are subdivided into *M* groups. The grouping is performed uniformly throughout volume of the structure, with *M* proportional to the root of number of BFs (as a rule of thumb). In each iteration, except the first, we create one MBF using BFs that belong entirely to the MoM area. In each iteration, except the zeroth, for each group of patches, we create MBF using BFs that belong to that group (in (3) we use $b_{lk}^{(i)} = 1$ if BF entirely belongs to the group, $b_{lk}^{(i)} = 1/L$ if BF belongs to L different groups, and $b_{lk}^{(i)} = 0$ otherwise). Particularly, each BF that belongs to both MoM area and PO area ("bridge" BF) is introduced as a single MBF in the first iteration (note that this is only appearance for these BFs).

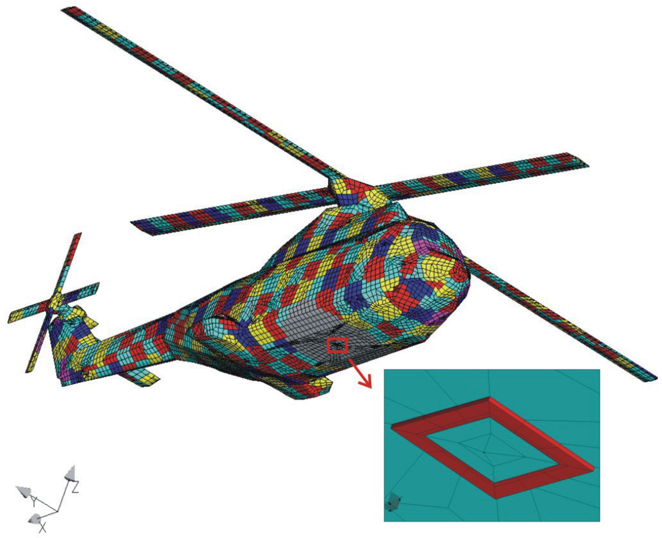

Fig. 1. Model of MPA on the helicopter, with 12022 patches, 95730 BFs, 4λ MoM area, and 698 groups of patches in PO area

The model of the helicopter with MPA mounted on its floor, shown in Fig. 1 (enlarged MPA is shown on the inset picture), has MoM area (gray patches) accommodated in a sphere (centered at MPA) which radius is four wavelength (4λ), and has 698 groups of patches (neighboring groups are differently colored) in PO area. Groups are distributed uniformly throughout the volume of the model. The groups do not contain sharp edges. We also created models with 342, 1345, and 2694 groups (all of them look similar, but with different size of the groups).

As a measure of convergence we use normalized Residuum

$$R_{\text{norm}}^{(n)} = \frac{R^{(n)}}{\frac{1}{N}\sum_{j=1}^{N}\left|v_j\right|^2}, \tag{15}$$

which is 0 for MoM solution and is 1 if all coefficients a_k in (1) are zero.

As we see in Fig. 2, Residuum decreases with iterations for all models. Convergence, though, is not uniform – it is the best at the beginning of the iterative procedure.

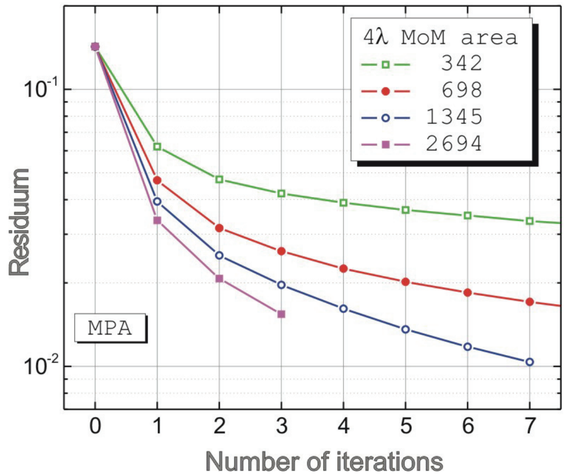

Fig. 2. Residuum as a function of Number of iterations

Changing size of MoM area to 2λ and to 8λ, while keeping number of groups close to 698 (711 groups for 2λ model, and 666 groups for 8λ model) just slightly shifts this curve up or down. This is shown in Fig. 3.

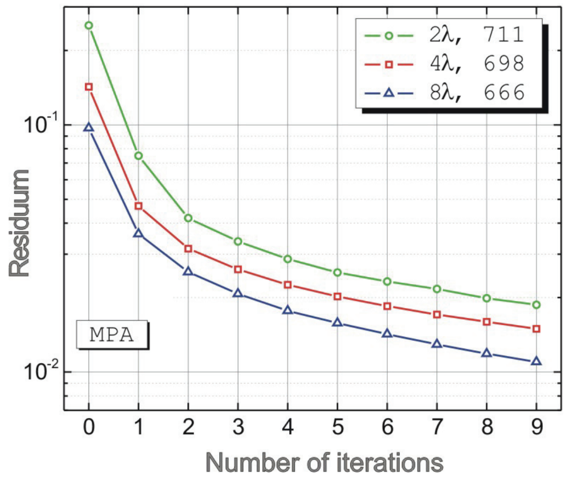

Fig. 3. Residuum as a function of size of MoM area

We can also see that models with higher number of groups have lower Residuum after the same number of iterations. However, if we look Residuum as a function of number of MBFs in Fig. 4, we see that "efficiency" (number of MBFs for certain Residuum) of different models depends on the wanted Residuum. Residuum as a function of CPU time is shown in Fig. 5. Note that CPU time for full MoM analysis on the same desktop PC (processor Intel Quad Core 2,67GHz, RAM 4 GB, graphics nVidia GTX 560) is about 5,5 hours. Since we calculate MoM matrix in each iteration, raw by raw, the memory occupancy depends solely of number of MBFs. Looking at Fig. 4, we can see that we work with number of MBFs that is at least order of magnitude lower than number of MoM BFs. Although we describe convergence by Residuum, it is an integral measure, whereas one is mostly interested in operative values of his antenna, such as gain and radiation pattern.

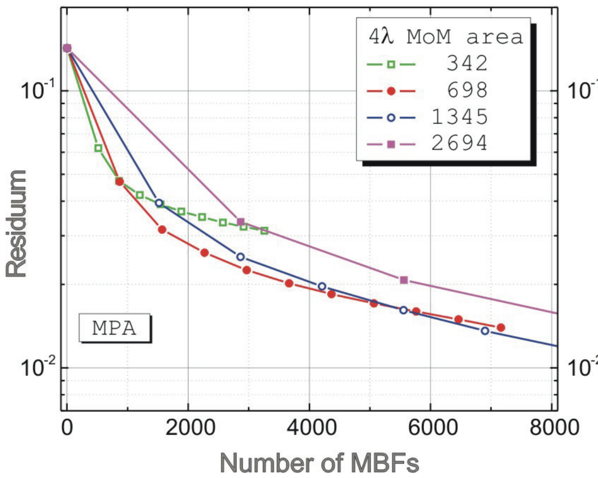

Fig. 4. Residuum as a function of Number of MBFs

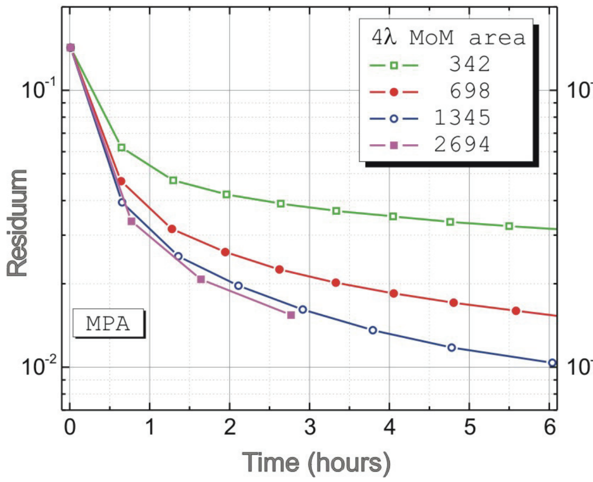

Fig. 5. Residuum as a function of CPU time

In Figs. 6-9 are shown gains obtained using PDM solution of model in Fig. 1 after 0, 1, 2 and 7 iterations, compared to gains obtained using MoM solution. The gains are calculated in plane $\phi = 0$ (ϕ is calculated from $+x$-axis, and θ is calculated from xy-plane). Iteration 0 is initial solution – essentially, it is MoM solution for extracted MoM area. Iteration 1 includes both bridge BFs and PO area BFs, whereas starting from iteration 2 we constantly add one MBF from MoM area and M MBFs from PO area. We see that the first iteration significantly improves the main lobe, whereas other iterations improve the side lobes. After 7 iterations (Residuum about 0.02) we have very good agreement with MoM solution. The effect of reducing the MoM area to 2λ on initial solution is shown in Fig. 10 – both the main lobe and the side lobes have larger deviation from MoM solution, but the levels remain practically the same. The similar thing, only in opposite direction, happens by expansion of MoM area to 8λ, as shown in Fig. 11.

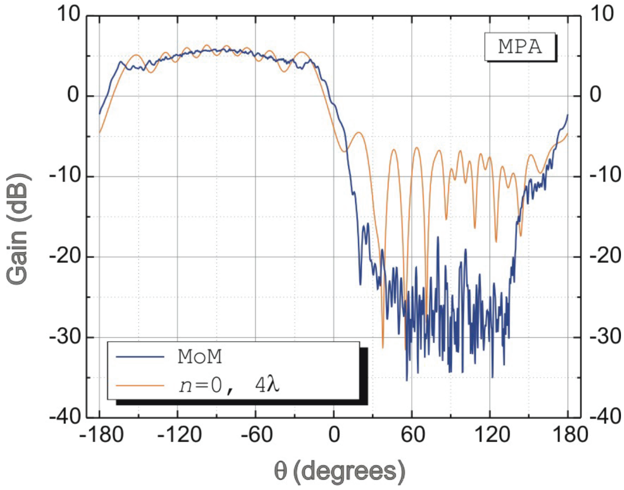

Fig. 6. Gain, Mom vs PDM solution of 4λ model, iteration 0

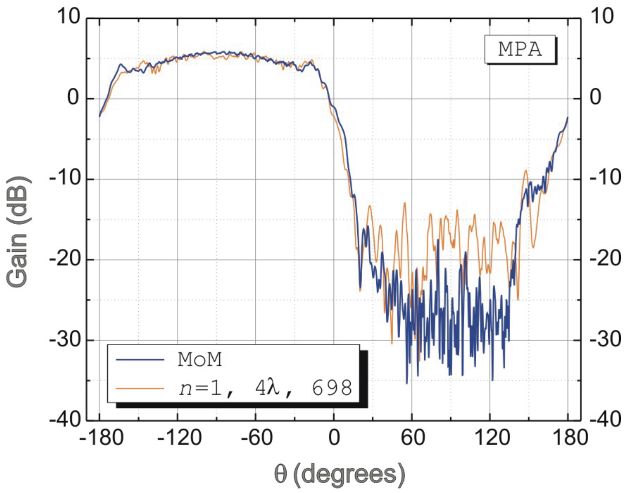

Fig. 7. Gain, Mom vs PDM solution of 4λ model, iteration 1

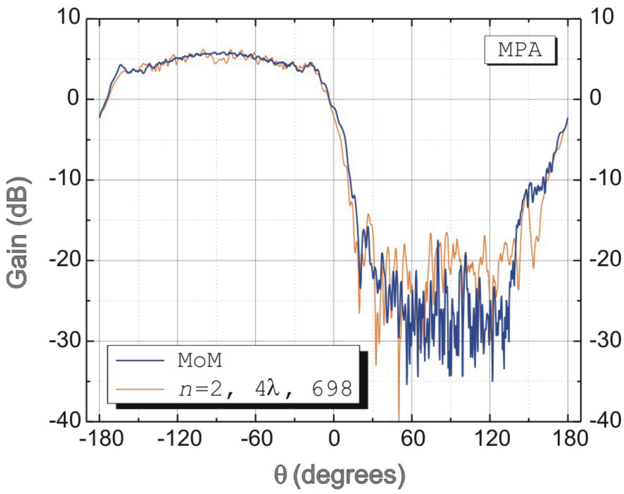

Fig. 8. Gain, Mom vs PDM solution of 4λ model, iteration 2

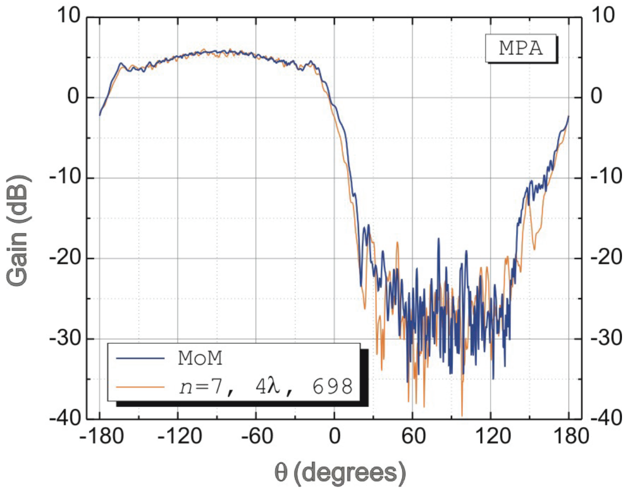

Fig. 9. Gain, Mom vs PDM solution of 4λ model, iteration 7

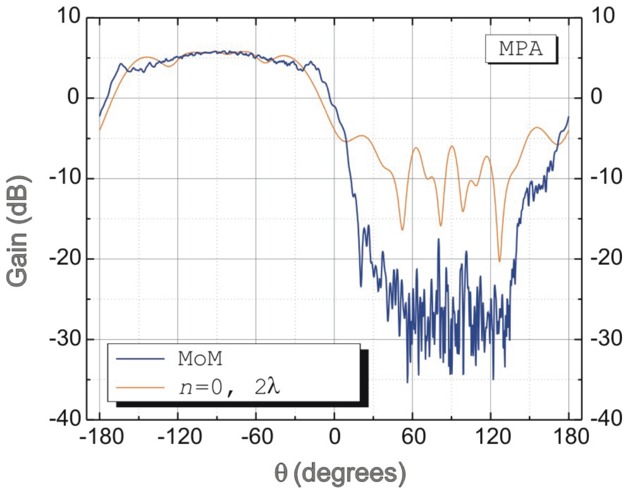

Fig. 10. Gain, Mom vs PDM solution of 2λ model, iteration 0

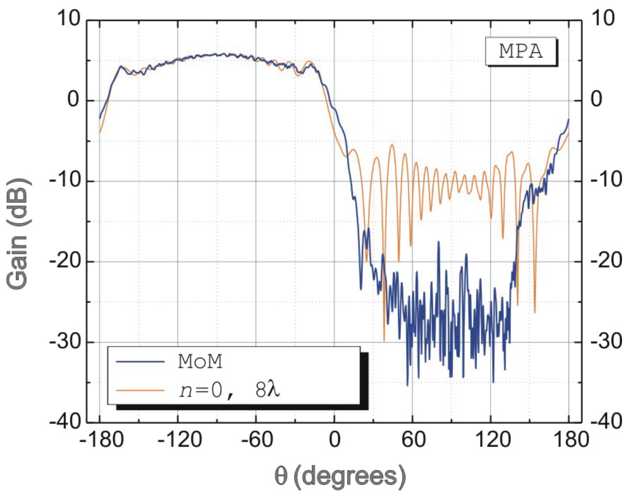

Fig. 11. Gain, Mom vs PDM solution of 8λ model, iteration 0

The second example is half-wavelength dipole antenna positioned quarter wavelength from the floor of the perfectly conducting airplane, 61 wavelengths long. The airplane's nose is directed along x-axis of Descartes coordinate system, whereas z-axis is orthogonal to airplane's floor and directed from it. The airplane is modeled using 13072 surface bilinear patches. Second order BFs are predominantly used, resulting in totally 104279 BFs. The model of the airplane with dipole antenna, shown in Fig. 12 (enlarged dipole is shown on the inset picture), has MoM area (gray patches) accommodated in a sphere (centered at the dipole) which radius is four wavelength (4λ), and has 316 groups of patches (colored) in PO area. We also created models with 665, 1320, and 2605 groups (all of them look similar, but with different size of the groups).

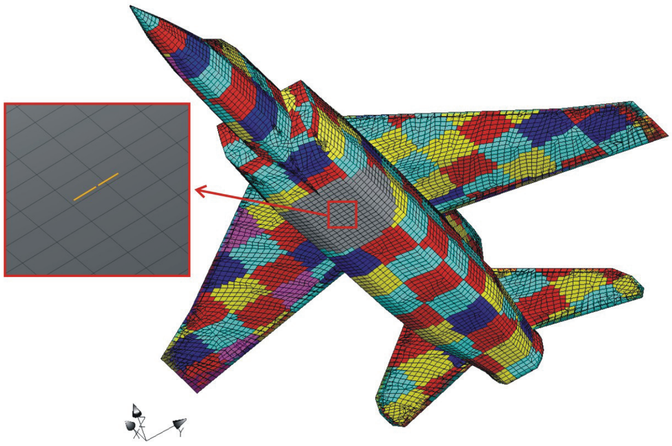

Fig. 12. Model of the dipole on the airplane, with 13072 patches, 104279 BFs, 4λ MoM area, and 316 groups of patches in PO area

Residua for these models, as a function of number of iterations, are shown in Fig. 13. As we can see, these residua are from two to three orders of magnitude smaller (batter) than those for helicopter models. In order to determine reason for such discrepancy, let as first look at the residua for three models with similar number of groups (around 316) and different size of MoM area – defined by spheres of 2λ (319 groups), 4λ (model in Fig. 12) and 8λ (306 groups), shown in Fig. 14. We can see that initial solution (iteration 0) for these models differs significantly – 0,034 for 2λ model, 0,0075 for 4λ model, and 0,0017 for 8λ model.

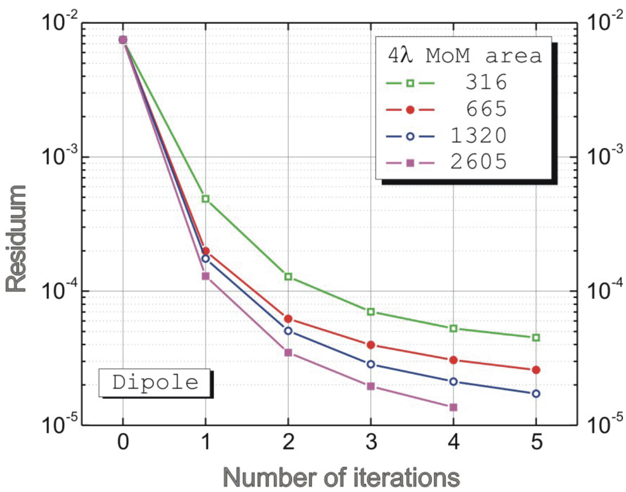

Fig. 13. Residuum as a function of Number of iterations

The models with larger MoM areas then preserves this advantage trough the iterations. However, as seen in Fig. 14, the convergence is better for models with smaller MoM area. The models with larger MoM area have very good initial solution, and it's hard to improve something that is already good. In Figs. 15-17 are shown gains obtained using PDM solution of models 2λ, 4λ, and 8λ in 0th iteration, compared to gains obtained using MoM solution. The gains are calculated in plane $\phi = 0$ (the airplane symmetric plane). Obviously, the change in the MoM area size have much more influence here than with MPA on the helicopter. Enlarging MoM area (from 2λ to 8λ) in certain degree improves the shape of the main lobe, but, in much larger extent, improves side lobes, both in shape and level. So, it seems that all important things in the analysis of the airplane models come in the vicinity of the dipole. MPA distributes its influence in wider space, so it is hard to "catch" all these interactions in small number of iterations. For dipole antenna, these interactions are "caught" fast. The gains after 1st iteration for 2λ and 4λ models are shown in Figs. 18 and 19. Gain for 2λ is now much better, for 4λ excellent, and for 8λ (not shown here) is almost perfect match with MoM.

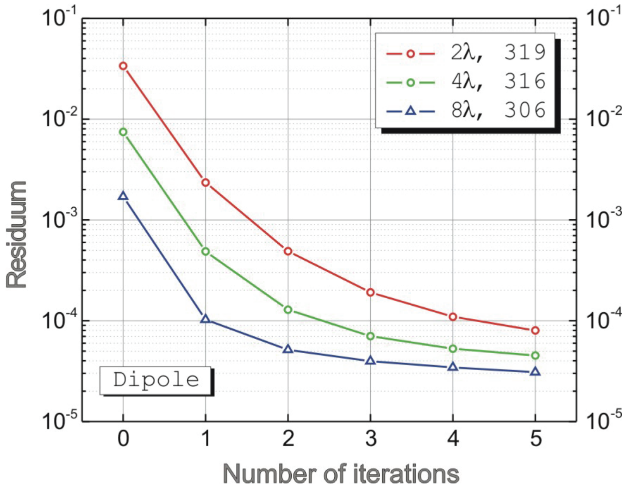

Fig. 14. Residuum as a function of MoM area size

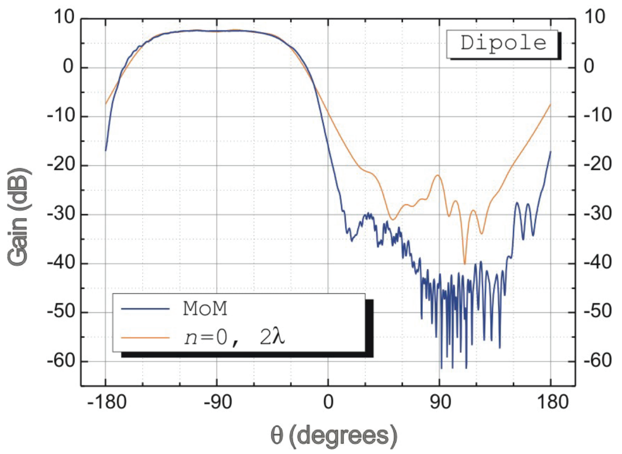

Fig. 15. Gain, Mom vs PDM solution of 2λ model, iteration 0

It is clear that number of MBFs here is extremely small (practically, we found perfect solution in single iteration) – about two orders of magnitude smaller than number of MoM BFs.

Finally, let as look how CPU time depends on number of iterations, as shown in Fig. 20. For smaller number of groups and smaller number of iterations, the dependence is practically linear. For large number of groups second, third and higher order of dependence arise, as predicted in [9].

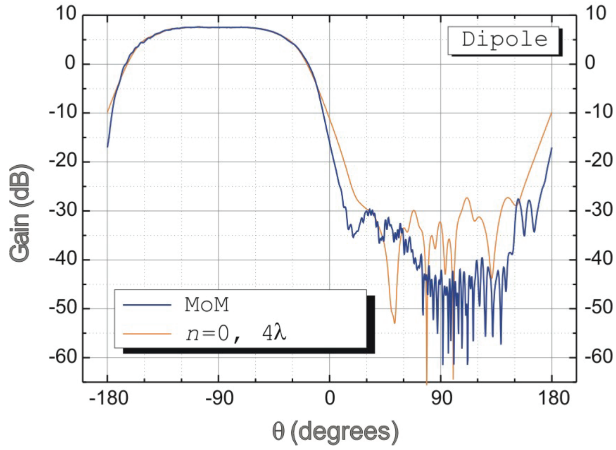

Fig. 16. Gain, Mom vs PDM solution of 4λ model, iteration 0

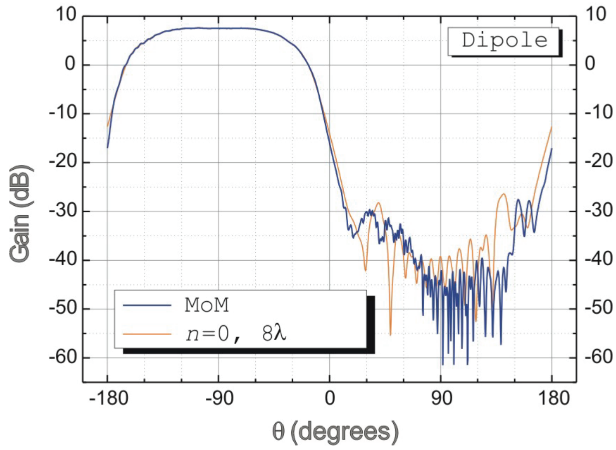

Fig. 17. Gain, Mom vs PDM solution of 8λ model, iteration 0

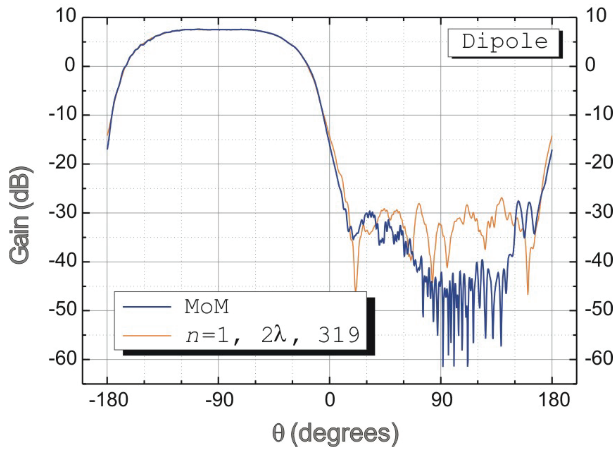

Fig. 18. Gain, Mom vs PDM solution of 2λ model, iteration 1

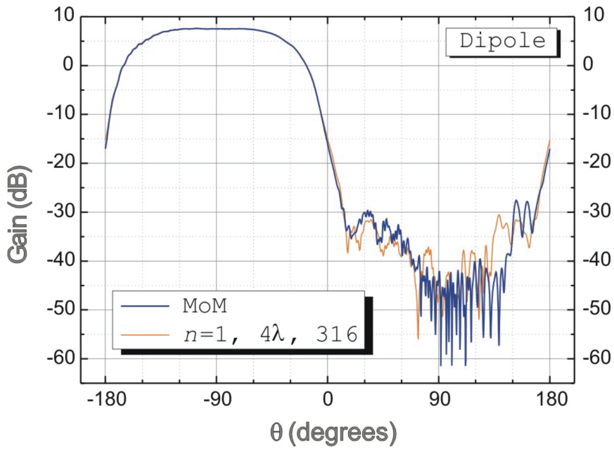

Fig. 19. Gain, Mom vs PDM solution of 8λ model, iteration 1

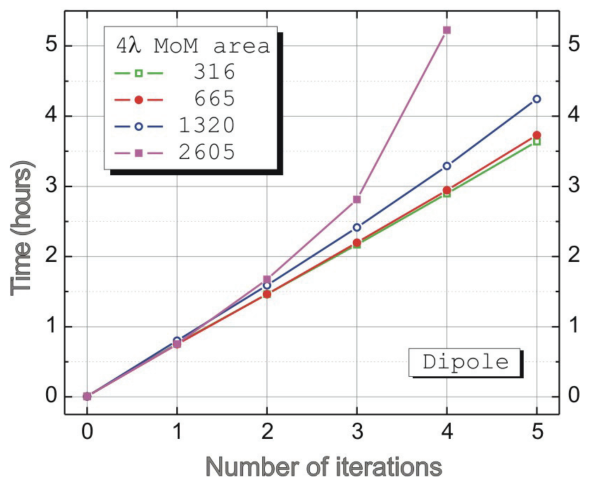

Fig. 20. CPU Time as a function of Number of iterations

IV. CONCLUSION

In this paper we presented PDM method (Physical optics Driven Method of moments) applied to antenna problems. We found that pure metal structures converge faster than composite metallic and dielectric structures. Numerical example shows good agreement with MoM solution, with reduction in memory occupancy from one to two orders of magnitude, and moderate reduction in CPU time. In this way PDM enables by two orders electrically larger problems to be solved on the same desktop PC, compared to classical MoM analysis.

ACKNOWLEDGEMENT

This work was supported by the Serbian Ministry of Education, Science, and Technological Development under grant TR-32005.

This is an extended version of the paper "Electromagnetic Analysis of Antennas on Large Platforms Using Physical Optics Driven Method of Moments," presented at the 11th International Conference on Telecommunications in Modern Satellite, Cable and Broadcasting Services - TELSIKS 2013, held in October 2013 in Niš, Serbia.

REFERENCES

[1] R. F. Harrington, *Field computations by moment methods.* New York: MacMillan, 1968.

[2] T. J. Kim and G. A. Thiele, “A hybrid diffraction technique-General theory and applications,’’ IEEE Trans. Antennas and Propagat., vol. AP-30, pp. 888-897, Sept. 1982.

[3] U. Jakobus and F. M. Landstorfer, “Improved PO-MM hybrid formulation for scattering from three-dimensional perfectly conducting bodies of arbitrary shape,” IEEE Trans. Antennas Propag., vol. 43, no. 2, pp. 162–169, Feb. 1995.

[4] R. Coifman, V. Rokhlin, and S. Wandzura, “The fast multipole method for the wave equation: A pedestrian prescription,” IEEE Antennas Propagat. Mag., vol. 35, no. 3, pp. 7–12, June 1993.

[5] J. M. Song, C. C. Lu, and W. C. Chew, “Multilevel fast multipole algorithm for electromagnetic scattering by large complex objects,” IEEE Trans. Antennas Propagat., vol. 45, pp. 1488–1493, Oct. 1997.

[6] J. Shaeffer, “Direct Solve of Electrically Large Integral Equations for Problem Sizes to 1 M Unknowns,” Antennas and Propagation, IEEE Transactions on , vol.56, no.8, pp.2306-2313, Aug. 2008.

[7] V. V. S. Prakash and R. Mittra, "Characteristic basis function method: A new technique for efficient solution of Method of Moments matrix equations," Microwave and Optical Technology Letters, Vol. 36, No. 2, pp. 95-100, Jan. 2003.

[8] L. Matekovits, V. A. Laza, and G. Vecchi, "Analysis of large complex structures with the synthetic-functions approach," IEEE Transactions on Antennas and Propagation, Vol. 55, No 9, pp. 2509-2521, Sep. 2007.

[9] M. Tasic and B. Kolundzija, “Efficient Analysis of Large Scatterers by Physical Optics Driven Method of Moments,” *Antennas and Propagation, IEEE Transactions on*, vol.59, no.8, pp.2905-2915, Aug. 2011.

[10] M. Tasic and B. Kolundzija, “Physical optics driven method of moments based on adaptive grouping technique,” Microwave Review, vol. 18, no. 2, pp. 2-7, Belgrade, December 2012.

[11] M. Tasić, and B. Kolundžija, “Elektromagnetska analiza električki velikih metalno-dielektričnih rasejača korišćenjem metode momenata vođene fizičkom optikom”, *Zbornik radova 57. ETRAN Konferencije*, 3-6. juna 2013, Zlatibor, Srbija, pp. AP1.6.1-5.

[12] B. Kolundzija, M. Tasic, D. Olcan, D. Zoric, and S. Stevanetic, “Advanced techniques for efficient modeling of electrically large structures on desktop PCs, “Applied Computational Electromagnetics Society Journal, *Special Issue on Computational Electromagnetics Workshop*, CEM 11, vol. 27, no. 2, February 2012, pp. 123-131.

[13] M. Tasić, and B. Kolundžija, "Electromagnetic Analysis of Antennas on Large Platforms Using Physical Optics Driven Method of Moments," *TELSIKS 2013, Proceedings of Papers*, Volume 2, pp. 433 - 436, Nis, Serbia, 2013.

[14] B. Kolundzija and A. Djordjevic, *Electromagnetic modeling of composite metallic and dielectric structures*, Norwood, USA: Artech House, 2002.

[15] *WIPL-D Pro v10.0, 3D EM solver*, http://www.wipl-d.com, 2012.